doi:10.1006/geno.2002.6831, available online at http://www.idealibrary.com on IDEAL **Article**

Ovol2, a Mammalian Homolog of *Drosophila ovo*: Gene Structure, Chromosomal Mapping, and Aberrant Expression in Blind-Sterile Mice

Baoan Li,[1] Qian Dai,[1] Ling Li,[1] Mahalakshmi Nair,[1] Douglas R. Mackay,[1] and Xing Dai[1,2,*]

[1]*Department of Biological Chemistry,* [2]*Developmental Biology Center, University of California, Irvine, California 92697, USA*

[*]*To whom correspondence and reprint requests should be addressed. Fax: (949) 824-2688. E-mail: xdai@uci.edu.*

The *ovo* gene family consists of evolutionarily conserved genes including those cloned from *Caenorhabditis elegans*, *Drosophila melanogaster*, mouse, and human. Here we report the isolation and characterization of mouse *Ovol2* (also known as *movol2* or *movo2*) and provide evidence supporting the existence of multiple *Ovol2* transcripts. These transcripts are produced by alternative promoter usage and alternative splicing and encode long and short OVOL2 protein isoforms, whose sequences differ from those previously reported. Mouse and human *OVOL2* genes are expressed in overlapping tissues including testis, where *Ovol2* expression is developmentally regulated and correlates with the meiotic/post-meiotic stages of spermatogenesis. Mouse *Ovol2* maps to chromosome 2 in a region containing blind-sterile (*bs*), a spontaneous mutation that causes spermatogenic defects and germ cell loss. No mutation has been detected in the coding region of *Ovol2* from *bs* mice, but *Ovol2* transcription was dramatically reduced in testes from these mice, suggesting that *Ovol2* is expressed in male germ cells.

Key Words: *Ovol2*, *movo2*, *Ovol1*, *movo1*, *Drosophila ovo/svb*, testis, blind-sterile (*bs*), spermatogenesis

INTRODUCTION

OVO is a conserved family of zinc-finger proteins that seem to act downstream of the wingless (wg)/wnt signaling pathway and are required for the differentiation of specific cell types in multicellular organisms [1,2]. So far, three *ovo* family members have been functionally characterized. *Drosophila melanogaster ovo* and mouse *Ovol1* (also known as *movo1*) are required for germ cell and epidermal appendage differentiation [2–6], whereas mutations in *Caenorhabditis elegans ovo* do not produce apparent fertility or epidermal defects, but instead cause defects in hindgut (the counterpart of mammalian urogenital system, where defects are found in *Ovol1* mutant mice) [7].

Current evidence supports the notion that OVO proteins function as transcription factors to regulate gene expression in various differentiation processes [1,7–9]. *Drosophila ovo*, being the prototype of *ovo* genes, is the most extensively characterized. It is a complex locus encoding multiple transcripts generated by alternative promoter usage and alternative splicing [10,11]. These transcripts encode multiple protein isoforms, all containing four identical Cys2/His2 zinc fingers at their carboxy termini but different amino-terminal domains. Consequently, these OVO proteins function as either transcriptional activators or transcriptional repressors [2,9,12,13].

Like its fly relative, the mouse *Ovol2* gene also produces multiple transcripts. Two of the transcripts encode the same nuclear protein that binds DNA sequences similar to the *Drosophila* OVO recognition site [1], whereas the complete sequence of the third and largest transcript remains to be determined. All three *Ovol1* transcripts are detected in mouse testis, specifically in premeiotic and meiotic germ cells, and in skin, specifically in differentiating cells of the epidermis and hair follicles [6]. Ablation of *Ovol1* in mice leads to male germ cell degeneration and structural abnormalities in the hair shafts, but no obvious defect in the epidermis [6]. Although these results support the model that *ovo* function in germ cell and epidermal appendage differentiation is conserved from flies to mice, they likely do not uncover the full spectrum of *ovo* functions in mammals, as a single fly gene usually evolves into multiple mammalian homologs, and some of the defects of *Drosophila ovo* mutants (such as those observed in the female germ line) have not been observed in mice deficient for *Ovol1*.

Copyright © 2002 Elsevier Science (USA). All rights reserved.

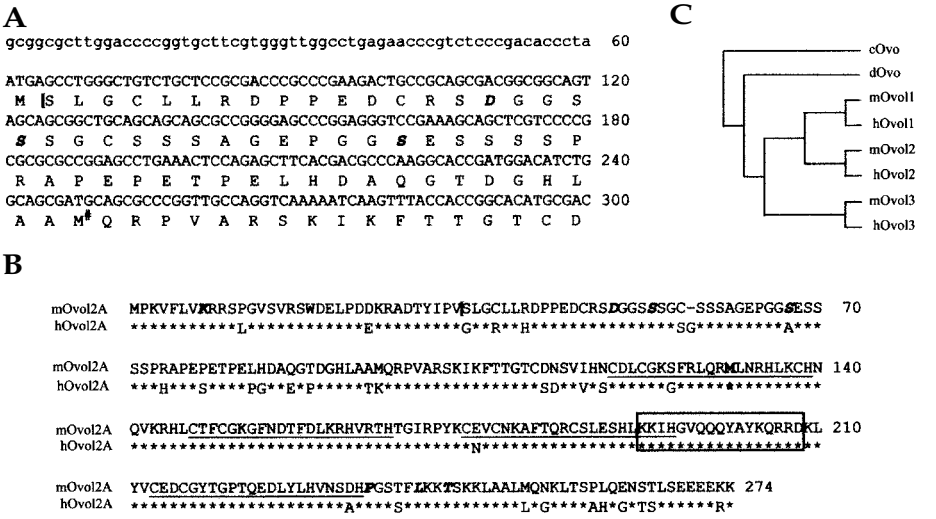

FIG. 1. Analysis of mouse and human *OVOL2* gene products. (A) The 5′ end sequences of the mouse *Ovol2*B cDNA and the deduced OVOL2B protein. The "#" symbol indicates the position of an internal methionine previously mistaken as the initiation codon [14]. (B) Deduced amino acid sequences of OVOL2A proteins in mouse (mOvol2A) and human (hOvol2A). The "*" symbol indicates amino acid identity. The four C2H2 zinc fingers are underlined. The predicted NLS sequences are boxed. Sequences common to mouse OVOL2A and OVOL2B start at the brackets in (A) and (B). Human OVOL2B starts at the internal methionine (bold). Shown in bold and italics are positions where our predicted sequence differs from the previously reported sequence [14]. (C) Phylogenetic analysis of OVO proteins. cOvo, *C. elegans* OVO (GenBank acc. no. AF134806); dOvo, *Drosophila* OVO (GenBank acc. no. X59772); mOvol1, mouse OVOL1 (GenBank acc. no. AF134804); hOvol1, human OVOL1 (GenBank acc. no. AF016045); mOvol2, mouse OVOL2 (GenBank acc. no. AY090537); hOvol2, human OVOL2 (GenBank acc. no. AK022284); mOvol3, mouse OVOL3 (GenBank acc. no. BF714064); hOvol3, human OVOL3 (GenBank acc. no. AD001527).

A second mouse *ovo* gene, *Ovol2* (also known as *movo2*) [6], exists, and cloning of two *Ovol2* cDNAs from a mouse testis library was reported [14]. Here we provide a corrected version of the mouse *Ovol2* cDNA sequences; report the isolation, characterization, and chromosomal localization of the mouse *Ovol2* gene; compare mouse and human *OVOL2* structure and tissue expression; and present evidence that mouse *Ovol2* is expressed in male germ cells and that this expression is developmentally regulated.

RESULTS

Characterization of Mouse *Ovol2* cDNAs and Sequence Comparison of the Putative Mouse and Human OVOL2 Proteins

Full-length mouse *Ovol2* cDNAs were obtained by compiling PCR-amplified cDNA fragments. Two classes of *Ovol2* cDNAs, differing in their 5′ end sequences, were obtained; however, these cDNAs differ considerably in size as well as in nucleotide sequence from those previously reported [14]. The most significant discrepancy is that our *Ovol2*B cDNA, ~ 1.2 kb in length, lacks an internal 177-bp fragment present in the reported sequence (Fig. 1A). RT-PCR on testis RNA using two different sets of primers detected single bands with sizes expected from our sequence (data not shown). This result indicates that the previously reported *Ovol2*B cDNA is from unprocessed RNA and includes a 177-bp intron, a notion further confirmed by sequencing mouse *Ovol2* gene (Fig. 2A).

The nucleotide sequences of our cDNAs differ from the reported sequences in multiple positions, and most of these translate into changes in amino acid identity (Figs. 1A and 1B). These differences were confirmed by sequencing relevant regions of the subcloned *Ovol2* genomic fragments. ORF analysis of the correct *Ovol2*A and *Ovol2*B cDNA sequences predicted an OVOL2A protein of 274 amino acids (Fig. 1B) and an OVOL2B protein of 241 amino acids (Fig. 1A). The putative OVOL2B protein is 62 amino acids longer than that previously reported [14] and contains an acidic/serine-rich domain (amino acids 35–90) and all four C2H2 zinc fingers, but lacks the highly charged N-terminal domain (amino acids 1–34, 35% charged) present in OVOL2A (Figs. 1 and 2A).

A GenBank search and BLAST analysis allowed us to identify several human EST and full-length cDNA sequences that share amino acid sequence identity to all *ovo* family members, but have the highest identity to mouse *Ovol2*. Like mouse *Ovol2*, these human *OVOL2* transcripts differ at their 5′ ends and can be divided into A and B classes accordingly (Fig. 2C). Furthermore, a subset of the transcripts contains additional 3′-UTR sequences. The encoded human OVOL2A protein shares 89% amino acid sequence identity with mouse OVOL2A (Fig. 1B). The zinc-finger domains of mouse and human OVOL2A are almost identical, sharing 98% amino acid sequence identity. Human *OVOL2*B also encodes a shortened protein isoform lacking N-terminal sequences present in human OVOL2A; in this case only three zinc fingers remain (Figs. 1B and 2C).

While *Drosophila* has only a single *ovo* gene, three distinct *ovo* genes (*Ovol1*, *Ovol2*, and *Ovol3*) exist in the mammalian genome. The mammalian OVO proteins share significant sequence identity with *Drosophila* OVO, but the similarity is restricted to the zinc-finger domains. Phylogenetic analysis based on the relatedness of the zinc-finger sequences of all known OVO proteins confirmed the orthologous relationship between mouse and human *OVOL2* (Fig. 1C). Furthermore, these phylogenetic relationships imply two gene-duplication

Copyright © 2002 Elsevier Science (USA). All rights reserved.

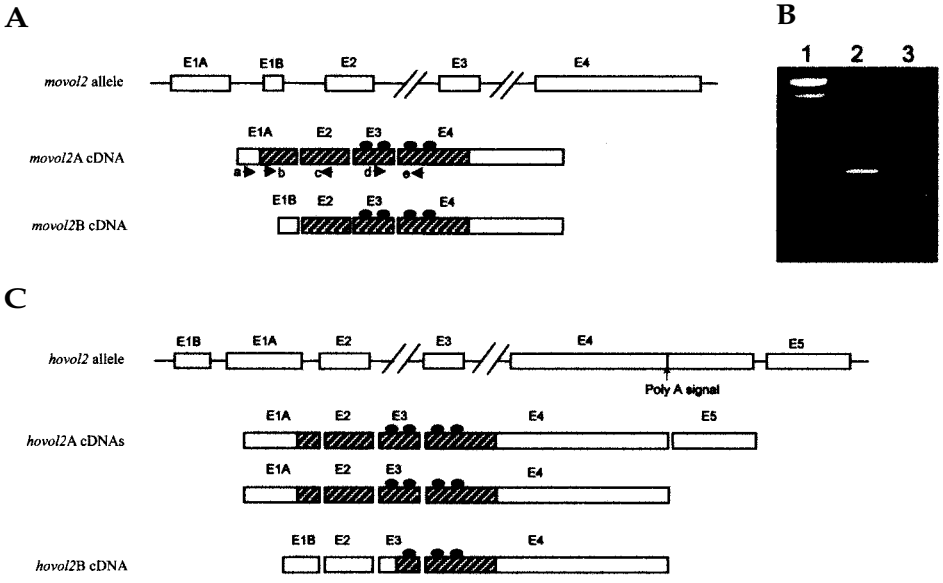

FIG. 2. Gene structure of mouse and human *OVOL2*. (A) Exon–intron structure of mouse *Ovol2* (*movol2*). Rectangular boxes represent exons (striped, coding sequences; open, noncoding sequences) and horizontal lines represent introns. Only exons are drawn to scale. The filled circle denotes a zinc finger. Arrows indicate positions and directions of primers used in RT-PCR: a, E1A1; b, WYF1; c, WYB4; d, F2; e, R2. The 177-bp intron between E1B and E2 was mistakenly included in the mouse *ovol2*B cDNA sequence previously reported [14]. (B) RT-PCR analysis of *Ovol2*A transcripts from mouse testis. Lane 1, 100-bp size marker; lane 2, primers E1A1 and WYB4; lane 3, primers WYF1 and WYB4. (C) Exon–intron structure of human *OVOL2* (*hovol2*).

events during evolution, leading to the present classes of mammalian *ovo* genes. That *Ovol1* and *Ovol2* are more closely related to each other than to *Ovol3* might provide clues to the functions of these mammalian *ovo* paralogs.

Gene Structure of Mouse and Human *OVOL2*

We isolated a BAC clone containing mouse *Ovol2* and determined the exon–intron organization of the gene. Mouse *Ovol2* consists of five exons, two of which (E1A or E1B) are alternatively used in *Ovol2*A and *Ovol2*B transcripts (Fig. 2A). RT-PCR using primer sets hybridizing to the 5′ end of *Ovol2*A cDNA and to E2 resulted in single PCR fragments (Fig. 2B), with sizes expected for *Ovol2*A transcripts. This result suggests that *Ovol2*B transcription initiates from an internal promoter, and the *Ovol2*A and *Ovol2*B isoforms are produced as a result of alternative promoter usage and alternative splicing, much like the multiple *Drosophila ovo* transcripts [9–11].

Two human BAC clones containing *Ovol2* were reported in GenBank (acc. nos. AL160411 and AL121585). Six exons exist in human *Ovol2* and, similar to the mouse gene, the first two are alternatively used in *Ovol2*A and *Ovol2*B transcripts (Fig. 2C). Exon 5 (E5) is only present in some transcripts: an alternative polyadenylation signal is present in E4 and its usage leads to the production of shorter transcripts. Exon/intron organization is similar in mouse and human *OVOL2*, as splice sites between E1A/E2, E2/E3, and E3/E4 are identical. Similar splice sites are also used in mouse *Ovol1* [6], further confirming that these mammalian *ovo* genes are derived from the same ancestor gene. The position of E1B is different between mouse and human: it is downstream of E1A in mouse *Ovol2* and upstream of E1A in human *OVOL2*. This difference accounts for the different sizes of the mouse and human OVOL2B proteins.

Tissue-Specific Expression of Mouse and Human *OVOL2*

Northern blot analysis using cDNA probes corresponding to either the coding sequences or sequences in the 3′-untranslated region common to mouse *Ovol2*A and *Ovol2*B detected *Ovol2* transcripts in a number of mouse tissues (Fig. 3A and data not shown). A major ~ 1.2-kb band was detected, consistent with the sizes of both cDNAs. This band is present most abundantly in testis, but also in skin, kidney, stomach, and intestine. Other smaller hybridizing bands were also observed, the most prominent of which is an ~ 1.1-kb band in brain. Furthermore, using RT-PCR, we detected *Ovol2* transcripts in total RNA prepared from adult mouse ovaries (Fig. 3B). This tissue distribution of mouse *Ovol2* transcripts appears broader than previously described, likely due to an underexposure of northern blots in that study [14]. Furthermore, our analysis indicates that mouse *Ovol1* and *Ovol2* are expressed in overlapping tissues including testis, skin, and kidney [6].

The expression of human *OVOL2* was examined using a probe common to human *OVOL2*A and *OVOL2*B transcripts. While both mouse and human *OVOL2* were expressed in overlapping tissues such as testis, human *OVOL2* displayed a broader tissue distribution spectrum than the mouse gene (Fig. 3C). Specifically, abundant levels of human *OVOL2* transcripts were detected in ovary, heart, and skeletal muscle, where mouse *Ovol2* expression was undetected.

Mouse *Ovol2* Is Expressed in Epidermal Keratinocytes Independent of Ca^{2+}-Induced Differentiation

The overlapping expression of mouse *Ovol2* and *Ovol1* in skin led us to ask whether *Ovol2*, like *Ovol1*, is also expressed in the epidermal compartment of skin. Indeed, *Ovol2* transcripts were detected in mouse keratinocytes derived from the skin

Copyright © 2002 Elsevier Science (USA). All rights reserved.

doi:10.1006/geno.2002.6831, available online at http://www.idealibrary.com on IDEAL

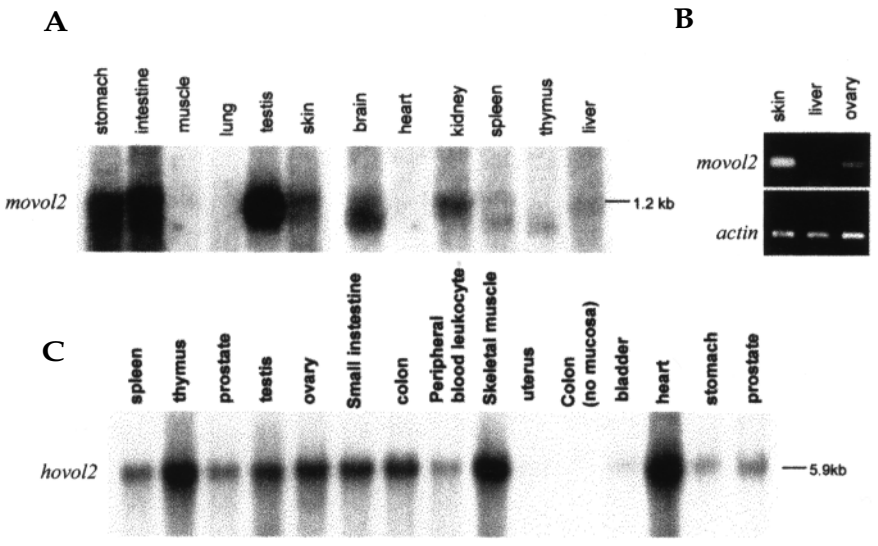

FIG. 3. Tissue-specific expression patterns of *OVOL2* in mouse and human. (A) Northern blot analysis of mouse tissue RNAs (Origene blots) using a probe containing sequences common to mouse *Ovol2*A and *Ovol2*B transcripts. (B) RT-PCR using primers F2 and R2 (Fig. 2A) common to mouse *Ovol2*A and *Ovol2*B transcripts (top), or using actin primers (bottom). (C) Northern blot analysis of human tissue RNAs (Clontech blots) using a probe containing sequences common to human *Ovol2*A and *Ovol2*B transcripts.

epidermis and cultured in low Ca^{2+} medium (Fig. 4). These keratinocytes, when treated with elevated levels of Ca^{2+}, can be induced to undergo morphogenetic and molecular changes mimicking terminal differentiation [15]. Distinct from mouse *Ovol1*, which shows a dramatic upregulation upon Ca^{2+} treatment [6], expression of mouse *Ovol2* appeared unchanged if not somewhat reduced upon Ca^{2+} induction. Despite this difference, the overlapping expression of *Ovol1* and *Ovol2* in epidermal keratinocytes suggests that the two *ovo* genes might have redundant functions in epidermis, which would explain the lack of an apparent epidermal defect in *Ovol1*-mutant mice [6].

Expression of Mouse *Ovol2*A and *Ovol2*B in Testis Is Developmentally Regulated

Despite the abundant expression of mouse *Ovol2* in testis, *Ovol1* mutant mice showed dramatic defects in spermatogenesis [6]. We carried out a detailed analysis of mouse *Ovol2* expression during prepubertal testis development, where the first, relatively synchronous round of spermatogenesis occurs. This process spans the first several postnatal weeks, and allows the germ-cell differentiation process to be temporally monitored [16] (Fig. 5A). Specifically, germ cells begin meiotic prophase between postnatal days 8 and 10, enter zygotene stage between days 10 and 12, and begin pachytene stage between days 12 and 14. The two meiotic divisions occur rather quickly, and haploid spermatids can be seen on day 18. We examined mouse *Ovol2* expression over the course of this time period using northern blot hybridizations. Consistent with previous observations [14], *Ovol2* transcripts were not detected in testis isolated from 1- to 2-week-old mice, but were abundantly present in testis from mice of 3–4 weeks (Fig. 5B). A closer examination revealed that *Ovol2* transcripts first appeared on day 15.5, when pachytene spermatocytes of meiotic prophase appear and accumulate, and were upregulated between days 16.5 and 17.5, when secondary spermatocytes and/or postmeiotic germ cells appear (Fig. 5C, top).

We next examined the temporal expression patterns of mouse *Ovol2*A and *Ovol2*B transcripts using isoform-specific probes. Both transcripts were present in developing testis and showed similar temporal patterns of expression (Fig. 5C). Whereas the level of *Ovol2*A transcripts peaks in adult testis, the level of *Ovol2*B transcripts peaks at 21 days after birth. This observation suggests that mouse *Ovol2*A and *Ovol2*B transcripts are co-expressed in late meiotic and/or postmeiotic germ cells, and that the fine-tuning of their expression levels relative to each other might be important to determine the final transcriptional output of mouse *Ovol2* target genes. The temporal expression of mouse *Ovol2* appears slightly later than that of mouse *Ovol1* (Q.D. and X.D., unpublished data), suggesting that *Ovol2* function might be required later than that of *Ovol1* in germ-cell differentiation.

Ovol2 Maps to a Chromosomal Region Containing the Blind-Sterile Mutation

To obtain additional clues about *Ovol2* function, we carried out FISH analysis and mapped *Ovol2* to the G band of mouse chromosome 2, in the vicinity of the *Ptpra* and *Bfsp1* loci (Fig. 6A). This region shares conserved synteny with human chromosome 20p11.2–p13, which contains human *OVOL2*.

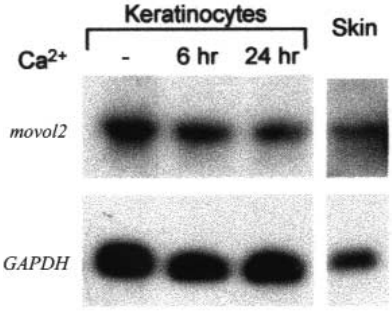

FIG. 4. Northern blot analysis of mouse *Ovol2* expression in keratinocytes. Total RNAs were prepared from mouse keratinocytes cultured in low Ca^{2+} medium (-) or treated with Ca^{2+} for hours (hr) indicated. A probe detecting both mouse *Ovol2*A and *Ovol2*B transcripts (*movol2*) was used. GAPDH was used as a control for loading.

Copyright © 2002 Elsevier Science (USA). All rights reserved.

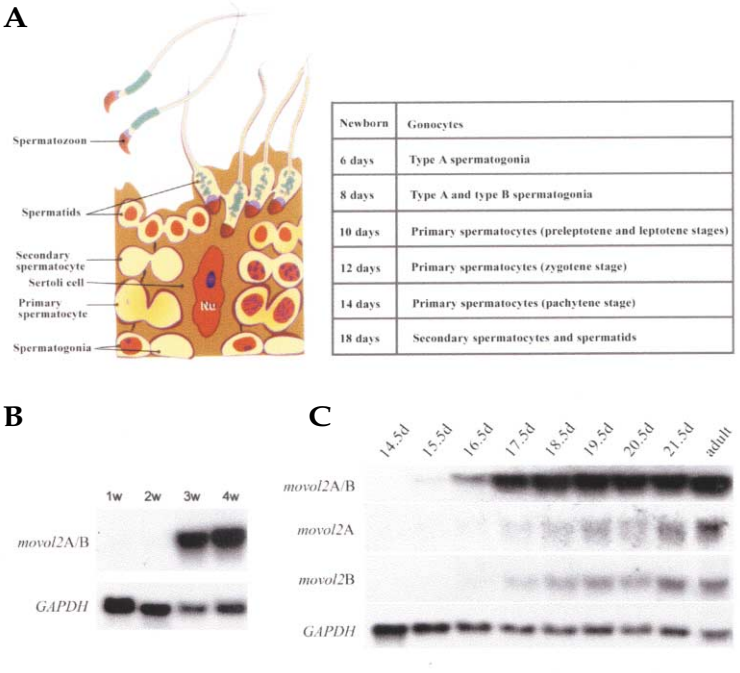

FIG. 5. Northern blot analysis of *Ovol2* expression during prepubertal testis development. (A) Diagram of the process of spermatogenesis. In the seminiferous tubules of testis, some of the mitotically active germ cells (spermatogonia) enter the program of differentiation to yield primary spermatocytes (corresponding to meiotic prophase and subdivided into several stages including preleptotene, leptotene, zygotene, pachytene, and diplotene) [24]. Primary spermatocytes undergo meiosis I to yield secondary spermatocytes, which then undergo meiosis II to yield haploid spermatids. Spermatids subsequently undergo morphological transformations to produce mature spermatozoon. The timing of the first appearance of germ cells of different differentiation stages in the first round of spermatogenesis is shown on the right [adapted from 16]. (B) Mouse *Ovol2* transcription in testis is upregulated at 3 weeks (w) after birth. (C) Abundant expression of mouse *Ovol2*A and *Ovol2*B transcripts correlates with the appearance of late meiotic/postmeiotic germ cells. Probes either common to mouse *Ovol2*A and *Ovol2*B transcripts (*movol2*A/B in B, C) or specific to each isoform (*movol2*A, *movol2*B in C) were used. Ages (weeks in B and days in C) at which testis samples were taken are shown at the top.

A spontaneous recessive mutation in mice, blind-sterile (*bs*), was mapped to a similar chromosomal region in the vicinity of *Bfsp1* [17,18]. Mice carrying this mutation display spermatogenic defects and germ-cell loss [19,20], a phenotype one might expect for mouse *Ovol2* mutations based on its abundant expression in testis. The stage when germ-cell defects are observed in *bs* mouse testis coincides with the timing of developmental upregulation of mouse *Ovol2*, further supporting a possible link between *Ovol2* and *bs*. To test if *bs* arises from mouse *Ovol2* mutations, overlapping genomic and cDNA fragments were obtained from *bs* mice (in AKR/129Sv background) by PCR and their sequences compared with that from AKR and 129Sv wild-type mice (Fig. 6B). No mutation was detected in *bs* mice within the regions examined, including all four exons and the two introns between E1A-E1B and E1B-E2. This result suggests that the mouse *Ovol2* coding sequences and the putative *Ovol2*B proximal promoter present in the intron between E1A and E1B are unaffected in *bs* mice.

We next examined whether *Ovol2* transcription might be compromised in *bs* mice. Although transcripts of expected sizes were present in testes from *bs* mice, the level of *Ovol2* transcription was reduced compared with that in the control mice (> 20-fold; Fig. 6C). However, this reduction is likely a consequence of male germ-cell depletion in *bs* mice, as the expression of mouse *Ovol1*—which is known to occur in male germ cells [6]—was also diminished in *bs* testis. Supporting this notion is our observation that levels of mouse *Ovol2* and *Ovol1* transcripts in *bs* kidney appeared comparable to that in the controls (data not shown). These results suggest that mouse *Ovol2*, like *Ovol1*, is expressed in male germ cells of the testis. Although we cannot rule out the possibility that *bs* arises from mutations in the upstream gene regulatory region of *Ovol2* that is responsible for its testis-specific activation, our results do not reveal a direct link between mouse *Ovol2* and *bs*.

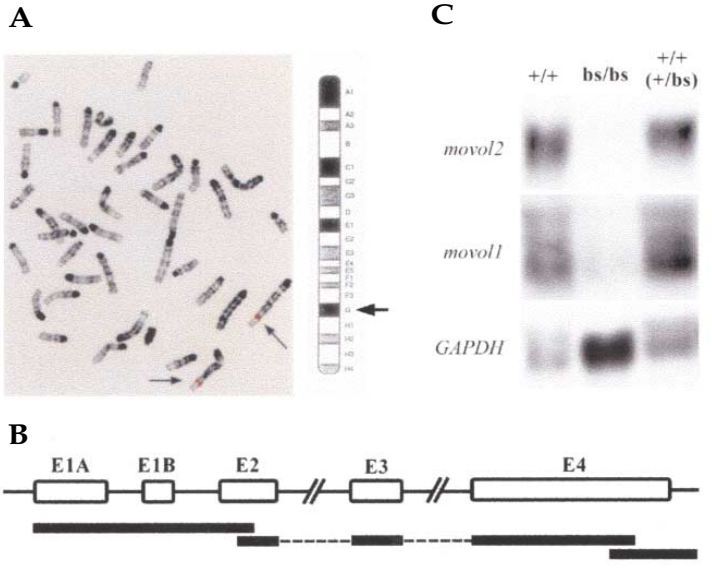

FIG. 6. Chromosomal mapping of mouse *Ovol2* and characterization of *Ovol2* sequence and expression in *bs* mice. (A) FISH analysis. Red dots (arrows) in the left panel represent hybridization signals obtained with a mouse *Ovol2*-containing BAC clone. On the right is the banding pattern of mouse chromosome 2. (B) Sequence analysis of mouse *Ovol2* in *bs* mice. Mouse *Ovol2* gene structure is shown at the top. Thick lines represent PCR fragments analyzed. For each fragment, at least two independent PCR reactions were carried out and the resulting fragments sequenced. (C) Northern blot analysis. Total testis RNAs were prepared from wild-type AKR mice (+/+), *bs* homozygous (*bs*/*bs*), and control littermates of *bs*/*bs* having either a +/+ or +/*bs* genotype.

Copyright © 2002 Elsevier Science (USA). All rights reserved.

doi:10.1006/geno.2002.6831, available online at http://www.idealibrary.com on IDEAL

DISCUSSION

Here, we have characterized *Ovol2*, a second mammalian homolog of *Drosophila ovo/svb*. As discussed above, three *Ovo* genes (*Ovol1*, *Ovol2*, and *Ovol3*) have been identified in the mouse genome, whereas *Drosophila* contains only a single *ovo* gene. The presence of mouse *Ovol3* is indicated by the identification of EST sequences (GenBank acc. nos. BF715622 and BF714064) that share extensive homology with *Ovol1* and *Ovol2*. Each mouse *Ovo* has a corresponding human ortholog (human *OVOL2* was previously known as zinc-finger protein 339), based on sequence homology. This orthologous relationship is further confirmed by their localization to chromosomal regions sharing conserved synteny. Mouse *Ovol1* maps to chromosome 19 [1] in a region sharing conserved synteny with human chromosome 11q13, where human *OVOL1* resides [21]; mouse *Ovol2* maps to chromosome 2 in a region sharing conserved synteny with human chromosome 20p11.2–p12, which contains human *OVOL2*. The chromosomal localization of mouse *Ovol3* has not yet been determined, but the fact that human *OVOL3* is localized to chromosome 19q13.1 suggests that mouse *Ovol3* likely resides on a region on mouse chromosome 7 that shares conserved synteny with human chromosome 19q13.1.

An interesting questions is how *ovo* function has evolved with the increase in *ovo* gene copy number. While *ovo* is required in *C. elegans* for urogenital development, it is required in *Drosophila* for germ-cell differentiation in both males and females and for epidermal denticle/cuticle differentiation. How are these primitive *ovo* functions partitioned between the mammalian *ovo* paralogs? Is there a separate role for each gene, are three genes working together, or is there a common pathway to carry out all of the biological functions of *ovo*? The tissue distribution of *Ovol2* transcripts is somewhat different from, but largely overlaps that of, *Ovol1*, raising the possibility of a partial functional overlap or interaction. The fact that a targeted disruption of *Ovol1* in mice led to defects in testis and kidney but not epidermis [6] (all three tissues express *Ovol2*) suggests that complete genetic redundancy is unlikely, and that the functional relationship between *Ovol1* and *Ovol2* might be complex and tissue-dependent. In this context, we note that loss of mouse *Ovol2* expression was observed in mouse *Ovol1*-mutant testis and that putative mouse OVOL1 binding sites were identified in the upstream promoter of *Ovol2*, suggesting that *Ovol2* acts downstream of *Ovol1* in germ-cell differentiation (B.L. and X.D., unpublished data). The temporal patterns of mouse *Ovol2* and *Ovol1* expression during prepubertal testis development support this model. In contrast, it seems that mouse *Ovol2* is not a target of *Ovol1* in keratinocytes given their differential expression during Ca^{2+}-induced terminal differentiation.

The developmentally regulated mouse *Ovol2* expression in male germ cells might be required for germ-cell differentiation, particularly at the meiotic and postmeiotic stages. Mouse *Ovol2* single-mutant and *Ovol1*/*Ovol2* double-mutant mice are being generated to determine the biological functions of mouse *Ovol2* and the possible genetic interaction between these two mouse *Ovo* genes. Although no information is currently available on the tissue expression of mouse *Ovol3*, human *OVOL3* ESTs were isolated from testis libraries, suggesting that *Ovol3* is also expressed in testis. Future work is needed to elucidate the functional relationship of *Ovol3* to *Ovol1* and *Ovol2* in mammalian development and differentiation, especially in germ-cell differentiation.

Are mouse and human *ovo* orthologs functionally equivalent? Our data reveal both similarities and differences between the tissue expression patterns of mouse and human *OVOL2*. While both genes are expressed in a number of epithelial tissues, human *OVOL2* is abundantly expressed in heart and muscle, whereas mouse *Ovol2* expression is undetected. The difference in tissue expression seems striking considering that the encoded proteins are quite similar in sequence (89% overall amino acid sequence identity) and suggests evolutionary changes in the *cis*-regulatory region of *Ovol2*. It is notable that interspecific differences in cuticle patterns between the different *Drosophila* species are entirely due to differences in *ovo/svb* expression patterns in the fly epidermis, presumably as a result of evolutionary changes in *ovo/svb* gene regulatory elements [22]. Whether a broadened expression spectrum from mouse to human translates into additional biological functions in human merits investigation. In any case, the overlapping expression of mouse and human *OVOL2* in epithelial tissues suggests that studies of the mouse gene will lead to a better understanding of *OVO* functions in human in normal and disease states.

Both mouse and human *OVOL2* encode two different putative protein isoforms, one of which is a shortened version of the other that lacks some N-terminal amino acids but contains the zinc-finger region. At least in mouse testis, *Ovol2*A and *Ovol2*B transcripts are co-expressed in differentiating germ cells, suggesting that the two protein isoforms coexist. The N-terminal domains of OVOL2A proteins are rich in charged and serine residues, characteristic of a transcription activation domain. As previously suggested [14], the shortened protein isoforms might act in a dominant negative fashion by virtue of their ability to bind cognate DNA sites, but inability to activate transcription. If this is the case, it will be reminiscent of the observation that the fly *ovo* gene encodes both transcriptional activators and repressors [2,9,12,13]. Expression of an activator and a dominant-negative repressor from a single regulatory gene is not unprecedented in mammals; an example of this includes the TCF/LEF family of transcriptional regulators [23]. It is possible that a delicate balance between OVOL2A and OVOL2B determines the final transcriptional output, a hypothesis currently under investigation. Given that relatively little is known about the gene expression programs during mammalian spermatogenesis, biochemical studies of OVOL2 proteins and identification of their downstream targets will provide insights into the control mechanisms and genetic pathways underlying this important biological process.

Copyright © 2002 Elsevier Science (USA). All rights reserved.

MATERIALS AND METHODS

Cloning and sequence analyses. Mouse *Ovol2*A and *Ovol2*B cDNAs were obtained by RACE on a Mouse Testis Marathon-Ready cDNA library (Clontech, Palo Alto, CA) according to the manufacturer's instructions, and RT-PCR on testis RNAs using primers designed based on a mouse *Ovol2* EST sequence (GenBank acc. no. W29556). A mouse BAC Down-To-The-Well genomic DNA library (Incyte Genomics, Palo Alto, CA) was screened using *Ovol2*-specific primers (F3, 5′-GCGACAAACTTTACGTGTGAGGATTGCG-3′, and B2, 5′-TGGCAGAATGACTGACAACTTTGGGGTGC-3′) according to manufacturer's instructions, and the *Ovol2*-containing BAC clone was then purchased from Incyte Genomics. Comparative PCR was performed using *Ovol2* cDNAs and the *Ovol2* BAC clone as templates to delineate the exon–intron organization of mouse *Ovol2*, and exon–intron boundaries were further confirmed by sequencing using standard dideoxy terminator methods. The exon–intron structure of human *OVOL2* was determined by comparing genomic and cDNA clones available in the database (GenBank acc. nos. AL160411, AL121585, AK022284, BC006148, BE791524, BE799878). Zinc-finger amino acid sequences of mouse and human OVOL2 proteins were aligned using CLUSTALW. For phylogenetic analysis, zinc finger amino acid sequences encoded by all *ovo*-related genes were aligned and tree calculated using CLUSTALW with *C. elegans ovo* sequence as an outgroup to root the tree.

RT-PCR. First-strand cDNAs were synthesized from total RNAs prepared from frozen tissues using SuperScript Reverse Transcriptase (Gibco Invitrogen Corporation, Carlsbad, CA) according to the manufacturer's instructions. The following primers were used in the subsequent PCR reactions, and their positions are indicated in Fig. 1A: a, E1A1, 5′-GAGAGTACCGAGCAACGC-3′; b, WYF1, 5′-CCCACCATGCCCAAAGTCTTTCTGGTAG-3′; c, WYB4, 5′-GGCGTCGTGAAGCTCTGGAGTTTCAG-3′; d, F2, 5′-GTGGCAAGAGCTTC-CGCCTGCAG-3′; e, R2, 5′-GGTCACTGTTCACATGCAGATACA-3′.

Northern blot analysis. Northern blots containing poly(A)$^+$ RNA from various adult mouse tissues were purchased from Origene (Rockville, MD). Human tissue blots were purchased from Clontech. For all other blots, total RNAs were isolated from frozen tissues using TRIzol Reagent (Gibco) according to the manufacturer's instructions, and 20 μg total RNA was loaded in each lane. Mouse keratinocytes were cultured and induced to differentiate by Ca^{2+} treatment [6]. The *bs* homozygous mice (*bs*/*bs*, on an AKR/129Sv background) were purchased from The Jackson Laboratory together with control littermates (+/+ or +/*bs*) and aged-matched wild-type AKR controls (+/+). Testes were taken from these mice at 8 weeks of age for RNA preparation.

The following probes were used for hybridization to RNA blots: a 320-bp PCR fragment containing sequences in E2 and E3 of mouse *Ovol2* (present in both *Ovol2*A and *Ovol2*B transcripts; Fig. 2A), a 106-bp PCR fragment containing the sequence of mouse *Ovol2* E1A (specific to mouse *Ovol2*A), a 179-bp *Sac*II–*Nar*I genomic fragment containing the sequence of mouse *Ovol2* E1B (specific to mouse *Ovol2*B), and a 310-bp *Pvu*II fragment containing E2 sequence of human *OVOL2* (present in both human *Ovol2*A and *Ovol2*B transcripts; Fig. 2C).

Chromosomal localization. The mouse *Ovol2*-containing BAC clone was used as a probe in FISH analysis done as described [1].

ACKNOWLEDGMENTS

We thank Judith Fantes for technical assistance with FISH; Christopher Schonbaum and Diane Bridge for help with the phylogenetic analysis; Elaine Fuchs (University of Chicago) for support and guidance; and Anthony Mahowald and Christopher Schonbaum (University of Chicago) for introducing us to ovo. This work was supported by the NIH Research Grant R01 AR47320 and the March of Dimes Basil O'Connor Grant #5-FY00-547 awarded to X.D.

RECEIVED FOR PUBLICATION MARCH 28; ACCEPTED JUNE 19, 2002.

REFERENCES

1. Li, B., *et al.* (2002). The LEF1/β-catenin complex activates *movo*1, a mouse homolog of *Drosophila ovo* gene required for epidermal appendage differentiation. *Proc. Natl. Acad. Sci. USA* **99:** 6064–6069.
2. Payre, F., Vincent, A., and Carreno, S. (1999). ovo/svb integrates Wingless and DER pathways to control epidermis differentiation. *Nature* **400:** 271–275.
3. Wieschaus, E., Nusslein-Volhard, C., and Jurgens, G. (1984). Mutations affecting the pattern of the larval cuticle in *Drosophila Melanogaster*. III. Zygotic loci on the X-chromosome and the fourth chromosome. *Wilhelm Roux's Arch. Dev. Biol.* **193:** 296–307.
4. Oliver, B., Perrimon, N., and Mahowald, A. P. (1987). The ovo locus is required for sex-specific germ line maintenance in Drosophila. *Genes Dev.* **1:** 913–923.
5. Oliver, B., Pauli, D., and Mahowald, A. P. (1990). Genetic evidence that the ovo locus is involved in Drosophila germ line sex determination. *Genetics* **125:** 535–550.
6. Dai, X., *et al.* (1998). The ovo gene required for cuticle formation and oogenesis in flies is involved in hair formation and spermatogenesis in mice. *Genes Dev.* **12:** 3452–3463.
7. Johnson, A. D., Fitzsimmons, D., Hagman, J., and Chamberlin, H. M. (2001). EGL-38 Pax regulates the ovo-related gene lin-48 during Caenorhabditis elegans organ development. *Development* **128:** 2857–2865.
8. Lu, J., Andrews, J., Pauli, D., and Oliver, B. (1998). Drosophila OVO zinc-finger protein regulates ovo and ovarian tumor target promoters. *Dev. Genes Evol.* **208:** 213–222.
9. Andrews, J., *et al.* (2000). OVO transcription factors function antagonistically in the Drosophila female germline. *Development* **127:** 881–892.
10. Garfinkel, M. D., Wang, J., Liang, Y., and Mahowald, A. P. (1994). Multiple products from the shavenbaby-ovo gene region of Drosophila melanogaster: relationship to genetic complexity. *Mol. Cell. Biol.* **14:** 6809–6818.
11. Mevel-Ninio, M., Terracol, R., Salles, C., Vincent, A., and Payre, F. (1995). ovo, a Drosophila gene required for ovarian development, is specifically expressed in the germline and shares most of its coding sequences with shavenbaby, a gene involved in embryo patterning. *Mech. Dev.* **49:** 83–95.
12. Mevel-Ninio, M., Fouilloux, E., Guenal, I., and Vincent, A. (1996). The three dominant female-sterile mutations of the Drosophila ovo gene are point mutations that create new translation-initiator AUG codons. *Development* **122:** 4131–4138.
13. Andrews, J., Levenson, I., and Oliver, B. (1998). New AUG initiation codons in a long 5′ UTR create four dominant negative alleles of the Drosophila C2H2 zinc-finger gene ovo. *Dev. Genes Evol.* **207:** 482–487.
14. Masu, Y., Ikeda, S., Okuda-Ashitaka, E., Sato, E., and Ito, S. (1998). Expression of murine novel zinc finger proteins highly homologous to Drosophila ovo gene product in testis. *FEBS Lett.* **421:** 224–228.
15. Hennings, H., *et al.* (1980). Calcium regulation of growth and differentiation of mouse epidermal cells in culture. *Cell* **19:** 245–254.
16. Bellve, A. R., *et al.* (1977). Spermatogenic cells of the prepuberal mouse. Isolation and morphological characterization. *J. Cell Biol.* **74:** 68–85.
17. Spence, S. E., *et al.* (1992). Genetic localization of Hao-1, blind-sterile (bs), and Emv-13 on mouse chromosome 2. *Genomics* **12:** 403–404.
18. Masaki, S., and Watanabe, T. (1994). The gene Bfsp1 for the lens fiber cell beaded-filament structural protein CP94 maps to mouse chromosome 2. *Genomics* **22:** 449–450.
19. Varnum, D. S. (1983). Blind-sterile: a new mutation on chromosome 2 of the house mouse. *J. Hered.* **74:** 206–207.
20. Sotomayor, R. E., and Handel, M. A. (1986). Failure of acrosome assembly in a male sterile mouse mutant. *Biol. Reprod.* **34:** 171–182.
21. Chidambaram, A., *et al.* (1997). Characterization of a human homolog (OVOL1) of the Drosophila ovo gene, which maps to chromosome 11q13. *Mamm. Genome* **8:** 950–951.
22. Sucena, E., and Stern, D. L. (2000). Divergence of larval morphology between Drosophila sechellia and its sibling species caused by cis-regulatory evolution of ovo/shaven-baby. *Proc. Natl. Acad. Sci. USA* **97:** 4530–4534.
23. Hovanes, K., *et al.* (2001). β-catenin-sensitive isoforms of lymphoid enhancer factor-1 are selectively expressed in colon cancer. *Nat. Genet.* **28:** 53–57.
24. Russell, L., Ettlin, R. A., Hikim, A. P. S., and Clegg, E. D. (1990). *Histological and Histopathological Evaluation of the Testis*. Cache River Press, Clearwater, Florida.

Sequence data from this article have been deposited with the DDBJ/EMBL/GenBank Data Libraries under accession numbers AY090537 (mouse Ovol2A cDNA) and AY090538 (mouse Ovol2B cDNA).

Copyright © 2002 Elsevier Science (USA). All rights reserved.